International Journal of Electrical and Computer Engineering (IJECE)
Vol. 15, No. 3, June 2025, pp. 2583~2598
ISSN: 2088-8708, DOI: 10.11591/ijece.v15i3.pp2583-2598

Developing gallium nitride-based inverters for high-performance photovoltaic integration in alternating current grids

Arsalan Muhammad Soomar, Piotr Musznicki
Faculty of Electrical and Control Engineering, Gdańsk University of Technology, Gdańsk, Poland

Article Info

Article history:

Received Jun 12, 2024
Revised Dec 12, 2024
Accepted Jan 16, 2025

Keywords:

Boost inverter
Phase locked loop control
Photovoltaic
Renewable energy
Sliding mode control

ABSTRACT

This study introduces a gallium nitride (GaN) based inverter optimized for alternating current (AC) grid integration, featuring a novel phase-locked loop (PLL) controller enhanced with sliding mode control (SMC). This hybrid PLL-SMC approach significantly improves power delivery from photovoltaic (PV) sources, achieving a total harmonic distortion (THD) of 5% and a maximum power point tracking (MPPT) efficiency of 99.1%. Extensive testing demonstrates the inverter's superior performance in grid synchronization, efficiency, and power quality compared to conventional inverters. The results underscore the critical role of advanced GaN-based inverters in enhancing solar energy utilization and advancing renewable energy integration into AC grids. This work sets a new benchmark for PV system integration, contributing to the broader adoption of renewable energy technologies.

Corresponding Author:

Arsalan Muhammad Soomar
Faculty of Electrical and Control Engineering, Gdańsk University of Technology
Gabriela Narutowicza 11/12, 80-233 Gdańsk, Poland
Email: Arsalan.muhammad.soomar@pg.edu.pl

1. INTRODUCTION

The commercialization of grid-connected photovoltaic (PV) inverter systems has significantly accelerated the growth of solar power generation. This expansion, coupled with the global adoption of renewable energy sources like wind and fuel cells, underscores the importance of developing compact, energy-efficient inverters, particularly for residential grid-connected systems with power capacities ranging from 2 to 10 kW [1]. Among various designs, central-type inverters have emerged as a cost-effective solution for medium to high-power grid-integrated solar installations. They offer superior maximum power point tracking (MPPT) efficiency, and their mass production drives down costs per kilowatt, making them an attractive option for advancing residential solar power systems [2]–[4]

The boost inverter, a traditional voltage source topology, is widely used in commercial and industrial applications, including PV-integrated systems for backup power and alternating current (AC) motor drives. It consistently delivers an output voltage higher than the direct current (DC) input, typically requiring a boost converter between the source and inverter. However, this setup can compromise size, weight, cost, and efficiency depending on power and voltage levels. The well-established voltage source configuration and its application in boost inverters, which can produce an AC voltage higher or lower than the DC input, depending on the duty cycle [5]–[7]. The integration of PV systems with the AC grid is crucial for maximizing energy utilization and advancing renewable energy technologies. However, modern inverters often face challenges related to inefficiency, poor power quality, and compatibility with gallium nitride (GaN) based devices [8].

This research aims to develop a GaN-based boost inverter that effectively integrates photovoltaic energy with the AC grid, ensuring high efficiency, improved power quality, and reliable performance. The proposed inverter addresses common grid integration challenges and is designed for cost-effectiveness, reliability, and flexibility, making it suitable for widespread deployment in residential and commercial settings across various solar systems and grid configurations. A significant advancement in the design and implementation of GaN-based inverters specifically tailored for PV systems integrated with AC grids. The study addresses the critical problem of inefficiency, poor power quality, and grid synchronization challenges that plague conventional inverters. By introducing a hybrid phase-locked loop (PLL) controller enhanced with sliding mode control (SMC), the proposed inverter achieves superior performance in MPPT efficiency and reduces total harmonic distortion (THD). The paper accurate examines the performance of the inverter across various scenarios, including standalone operation without grid connection, grid disconnection and reconnection, frequency disturbances, and amplitude changes in grid supply. These cases highlight the robustness and resilience of the proposed inverter design under real-world conditions. The research sets a new benchmark for PV system integration, contributing to the broader adoption of renewable energy technologies and supporting the sustainable development of energy systems globally.

2. METHOD

The boost converter is a DC-DC converter utilized in PV systems to elevate the voltage of the DC power generated by the PV panels to levels compatible with the grid or other loads. The duty cycle of the boost converter is adjustable to provide control, and it may incorporate protective features to prevent system damage [2]. The efficiency of the boost converter is a critical factor in PV system design, used in conjunction with an MPPT controller to optimize the energy output from the PV panels. Power inverters, which convert DC into AC, play an essential role in PV systems by transforming the DC power from PV panels into AC power necessary for grid connection or powering AC loads. Various control schemes optimize these inverters' performance and efficiency [3]. GaN transistors are preferred in power converters for renewable energy systems because of their superior efficiency, power density, switching speed, thermal performance, and potential cost-effectiveness [4].

This study incorporates a Cuk switching mode power supply (SMPS) and a sliding mode control scheme in the photovoltaic inverter design to achieve reliable closed-loop performance. This methodology enables the use of smaller, more reliable non-electrolytic capacitors. A prototype inverter was developed to test the design [5]. The research discusses an MPPT method based on adaptive sliding mode control. The proposed technique uses an adaptive sliding mode controller (ASMC) to drive a boost converter that connects the PV generator to the load. The efficiency of this technique is validated by simulation results using real data in MATLAB/Simulink, and the ASMC controller's durability and stability are tested under variable weather conditions [6]. Liu *et al.* [7] propose a two-mode control strategy for bidirectional power converters in AC/DC hybrid microgrids operating under weak grid conditions. They achieve stability by managing the short-circuit ratio, controlling voltage and current sources, and mitigating system inertia. Simulation results demonstrate this strategy's effectiveness. A robust non-linear controller for voltage source converters (VSCs) connected to unreliable AC networks. This controller, designed using feedback linearization technique, manages the active power and output voltage of grid-connected converters. It is capable of handling faults and sustaining performance under unexpected active power demands in highly unstable AC grid conditions. The controller's robustness is evaluated through time-domain simulations and eigenvalue analysis [9].

Microgrids are considered fundamental components of a smart grid, involving procedures and controls such as load sharing, fault isolation, and voltage matching. The paper reviews the four primary control strategies employed in microgrids and the challenges encountered during operation in both grid-connected and standalone modes. It also explores alternative strategies for microgrid integration and future research directions [10]. A boost converter links the PV panels to the load, and an inverter equipped with a proportional-integral (PI) controller converts the voltage from DC to AC. MATLAB/Simulink simulation results affirm the effectiveness of the suggested control [11], [12]. Photovoltaic systems operate based on the photovoltaic effect, where electron-hole pairs are generated in semiconductor materials upon photon absorption from sunlight. The separation of electrons and holes by an electric field within a solar cell produces voltage and electric current, transforming solar energy into electrical energy. PV systems use this mechanism to directly convert sunlight into power, employing semiconductor materials like silicon in solar panels to harness electrical energy from solar radiation. Due to technological advancements and reduced costs, photovoltaic systems have become more accessible and cost-effective, playing a crucial role in the global transition to renewable energy sources [13]–[15].

2.1. Principle operation

The photovoltaic effect in semiconductor materials leads to the creation of electron-hole pairs upon the absorption of sunlight, a key process for converting solar energy into electricity. Within a solar cell, an electric field separates these electrons and holes, generating voltage and current. PV systems capitalize on this phenomenon to produce electricity directly from sunlight, using silicon solar panels to convert solar radiation into electrical energy. Due to technological advancements and decreasing costs, PV systems have grown in popularity and affordability, making them a cornerstone in the shift toward renewable energy. They find widespread use in residential, commercial, and utility-scale applications. Essential components of a photovoltaic system include solar panels, inverters, charge controllers such as MPPT, batteries for backup power storage, and mounting structures. Solar panels function by absorbing sunlight and producing DC electricity. Inverters are critical as they convert this DC electricity into AC, which is suitable for use in homes and businesses. Charge controllers effectively regulate the voltage and current coming from the solar panels to safely charge batteries, preventing overcharging and extending battery life. Batteries store surplus electricity generated during peak sunlight hours for use at other times, enhancing the system's efficiency and reliability. Finally, mounting structures provide the necessary support and stability, allowing the solar panels to be installed securely and positioned optimally for maximum sunlight exposure.

2.2. Design of inverter

The initial stage of the converter presented in Figure 1 centers around the DC boost, utilizing a traditional boost converter setup. The boosted DC output is subsequently connected to a high electron mobility transistor (HEMT) based on GaN, which is regulated by a PLL. The PLL's primary function is to synchronize the inverter with the grid's AC voltage. The output from the PLL is then directed to the control block, where SMC is applied for Integration of energy produced from solar power can lead to disastrous distortion in voltage and current profile of the AC grid also it may lead to degrading the efficiency of the system [16]. This control strategy is responsible for managing the power delivery to all five switches in both the DC boost converter and the inverter section. Following the control phase, the output from the inverter passes through an LCL filter configuration, comprising an inductor-capacitor-inductor arrangement. The necessitates the deployment of LCL filters as a strategic approach to limit current harmonics effectively [17]. This setup is widely used in grid-connected inverters due to its effectiveness in minimizing grid interference and smoothing the output signal.

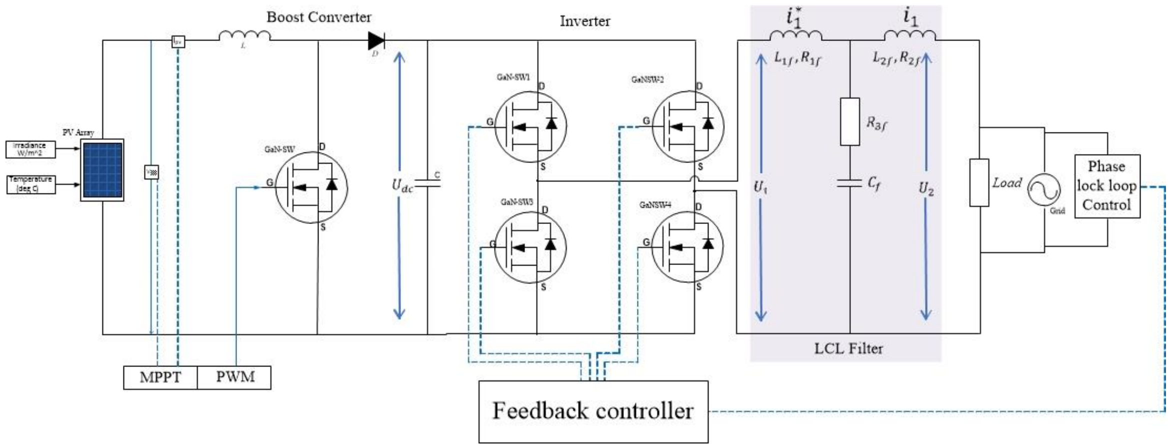

Figure 1. Schematic view of the GaN based inverter

The innovative aspect of the proposed boost inverter lies in its differential connection across the switches of the DC-AC converter to facilitate the DC to AC conversion. The output voltages from the DC-AC converter are sinusoidally modulated, as detailed in Figure 1. This modulation approach has been previously explored within the context of boost converters. The converters generate a unipolar voltage output, driven by the sinusoidal modulation, with each converter's modulation phase shifted by 180 degrees relative to the other. This phase shift maximizes the voltage excursion across the load. A differential connection across the converters is established, and by employing the averaging concept, the voltage relationship in continuous conduction mode is defined. Despite the presence of an AC sine wave at each end of the load, the differential DC voltage across the connection remains zero. The output voltage is determined through a specific formula, and the voltage gain for the boost inverter is inferred from the duty cycle when the converters are phased 180 degrees apart, as stipulated in (1). One intriguing characteristic to achieve is a zero-output voltage, with variations in the duty cycle around this point resulting in the generation of an AC voltage at the output terminal.

$$\frac{V_1}{V_{in}} = \frac{1}{1-D} \tag{1}$$

2.3. Development of a robust model of the inverter

The inverter's control scheme and schematic are illustrated in Figure 1, which also represents the switch feedback control implemented via PLLs. These PLLs, crucial for ensuring synchronization with the grid's frequency and phase, the model of the boost inverter has been configured in MATLAB/Simulink, showing the inverter connected to a load and the grid, controlled by a sliding mode controller. This schematic includes comprehensive components along with measurement and control units, which are essential for monitoring and managing the operation of this GaN-based inverter model.

The specific parameters of the designed converter are detailed in Table 1. These parameters play a critical role in the functionality and efficiency of the inverter, providing insights into its performance under various operational conditions. String configuration two parallel and six series.

Table 1. Parameter of the inverter design and components of the simulation

Parameters	Values
Solar panel power rating (Jinko Solar Co.)	
Maximum power of panel (W)	250.1
Open circuit voltage (Voc)	37.7
Short circuit current (Isc)	8.85
Maximum voltage (Vmp)	30.5
Panel current (Imp)	8.2
Irradiance (W/m^2)	1000
Temperature (oC)	25
Maximum power of solar	3,001.2
Maximum current	16.4
Maximum voltage	183
Boost converter	
Boost inductor	450 µH
DC-link capacitor	15.625 µF
Boost switching frequency	100 kHz
Feedback controller parameter	
Proportional gain (Kp1)	2.03
Proportional gain (Kd)	0.0002
Proportional gain (Kp2)	1
Integral gain (9Ki)	3,142
LCL filter	
Linveter	0.9 mH
Lgrid	0.89 mH
Filter capacitor	400 µF
Average output voltage	400 V
Vin	350
Delta I (Ripple current of inductor)	0.2%
Delta V (Ripple current of capacitor)	0.06%
Output current (Iout)	7.5
Output voltage (Vout)	400 V
Grid voltage (RMS)	220 V
Output power (W)	2,999

2.4. Design of LCL filter

A dual-loop control structure for single-phase shunt active power filters (SAPF) that incorporates feedforward control to mitigate grid voltage disturbances, complemented by a plug-in repetitive controller as the outer loop controller. The inner loop utilizes a PI controller to adjust the frequency response of the LCL filter, facilitating a quicker transient response and simplifying the design of the outer loop controller. The paper conducts a comprehensive analysis of the feedforward control's performance, assessing the stability and robustness of the dual-loop control system. Experimental results demonstrate the system’s effective steady-state performance, rapid transient response, efficient grid voltage attenuation, and resilience to variations in LCL filter parameters [15], [18].

The output of the inverter is characterized by its non-sinusoidal nature, containing additional harmonics that need filtering to eliminate spikes or other unwanted signals. For this purpose, the well-known LCL filter is employed, as illustrated in Figures 2(a) and 2(b) of the schematic diagrams. The LCL filter is commonly utilized for building and connecting inverters to the AC grid, favored for its ability to effectively suppress higher-order harmonics once the filter bandwidth and other parameters are properly configured [19]–[21].

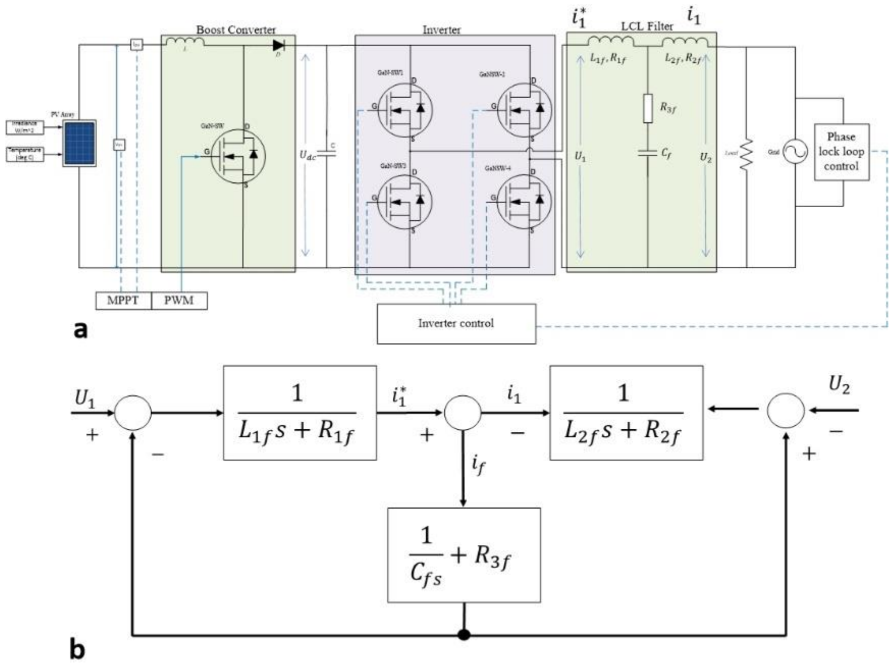

Figure 2. Schematic representation of a single-phase inverter with LCL filter (a) detailed circuit of a grid-connected single-phase inverter with LCL filter, and (b) block diagram representation of the LCL filter model

Here is a convenient formula for calculating the LCL filter capacitance (2) to (8) [22], [23]:

$$\frac{1}{C_f} = \frac{\lambda S_{grid}}{\Omega_0 U_{max}^2} \tag{2}$$

where, $\Omega_0 = 2\pi f_0$ is the frequency of the Grid, S_{grid} is the power absorbed by the inverter under rated circumstances, U_{max} is the grid voltage magnitude (peak value), and λ is the intended proportion of the LCL filter capacitance's absorption of inverter power. Here is the calculation for the input and output inductances of the LCL filter:

$$L_{1f} = \frac{U_{dc}}{6 f_{sw} \Delta I_{f,max}} \tag{3}$$

where U_{dc} is the DC link voltage value, f_{sw} is the inverter pulse width modulation switching frequency, $\Delta I_{f,max.}$ Is the greatest amount of filter current fluctuation caused by switching action, and r is the filter input/output inductance ratio, typically between 1/4 and 1/6.

$$L_{2f} = rL_{2f} \tag{4}$$

The above LCL filter is characterized by its resonance frequency.

$$\Omega_{res} = 2\pi f_{res} = \sqrt{\frac{L_{1f}+L_{2f}}{L_{1f}L_{2f}C_f}} \tag{5}$$

whereas following inequality condition must also be satisfied by the filter parameters

$$10f_0 < f_{res} < f_{sw}/2 \tag{6}$$

In order to minimize the main voltage/current harmonic at the frequency while also favorably attenuating the pulse width modulation (PWM) switching action. In order to minimize the main voltage/current harmonic at the frequency while also favorably attenuating the PWM switching action. $\Omega_0 = 2\pi f_0$. Finally, the series of resistance R_{3f} of the parallel capacitance branch is computed using the subsequent formula:

$$R_{3f} = \frac{2L_{res}}{C_f \Omega_{res}} \tag{7}$$

wherein L_{res} is the LCL filter damping at resonance frequency Ω_{res}. By choosing $\Omega_{res} > 0.5$, By making sure the LCL filter is dampened favorably at the resonance frequency, low-ripple LCL filter operation is determined. If the capacitive impedance is present at the principal harmonic frequency $1/(\Omega_0 C_f)$ takes on relatively large values (parameter λ << 1 in (2)), the capacitance current $i_f = i_1^* - i_1$ may be neglected concerning filter output current i_1, and the following form can be used to simplify the LCL filter transfer function model: Auxiliary PI controller for DC current suppression in single phase AC inverter current PR control.

$$G_{f(s)} = \frac{i_{1}(s)}{u_{1}(s) - u_{2}(s)} = \frac{1}{L_f s + R_f} = \frac{K_f}{T_f s + 1} \tag{8}$$

where $\mathrm{R_f = R_{1f} + R_{2f}}$ and $\mathrm{L_f = L_{1f} + L_{2f}}$ are the equivalent for filters and the constant for gain is $\mathrm{K_f = 1/R_f}$ and the time constant is $\mathrm{T_f = \frac{L_f}{R_f}}$. Respectively. The design of the LCL filters calculated with the mathematical derivation is shown in the equation.

2.5. Phase-locked loop integration

A PLL-based control method was proposed to integrate a grid-connected solar PV system more effectively, offering swifter grid integration and optimal system synchronization. Researchers developed a hybrid control mechanism that combines PI and phase-shift control to ensure the power quality of the grid. In this setup, the PLL plays a crucial role by controlling and synchronizing the inverter's firing angle. It provides control inputs to the sliding mode controller, which in turn manages the firing angles of the inverter and boost switches, as well as the regulation of both reactive and active power from the grid [24].

For single-phase systems, obtaining accurate grid voltage information is crucial. Traditional zero-crossing detection methods, although commonly used for this purpose, are impractical due to their sensitivity to noise. Consequently, an enhanced approach involving the use of two virtual PLL phases is required. Reference frame theory is applied here, positing that the single-phase voltage should be treated as a virtual two-phase voltage, with a 90-degree out-of-phase component to facilitate simpler control mechanisms. Based on this theory, a single-phase PLL system is structured in two stages: a two-phase generator and a phase controller, as depicted in Figure 3. This approach addresses the inherent limitations of single-phase systems and provides a robust framework for maintaining synchronization and stability in grid-connected solar PV systems.

- Two-phase generator: This block takes the utility voltage $V_{utility}$. It produces two signals: one that passes through an all-pass filter, yielding V_{qs}, and another that is used directly, V_{ds}. The all-pass filter likely ensures that V_{qs} are orthogonal to V_{ds}.
- Reverse Park transformation: This operation typically takes the orthogonal components V_{qs} and V_{ds} and transforms them into a rotating reference frame (d-q frame), resulting in a direct-axis voltage, V_{de}.
- Phase controller: The core of the PLL is where V_{de}, is fed into a proportional-integral (PI) controller. The PI controller aims to reduce the error between V_{de} and a reference value (which appears to be zero in this case). The output of the PI controller is an angular frequency deviation $\Delta\omega$.
- Integrator: The integration of the frequency deviation over time to estimate the phase angle $\hat{\theta}$, then fed back to the phase detector. In terms of transfer functions, the all-pass filter will have a transfer function $H_{ap}(s)$, where $_{(s)}$ is the complex frequency variable. The PI controller is expressed as (9) [25]:

$$H_{pi(s)} = K_p + \frac{K_i}{s} \tag{9}$$

where the proportional gain is K_p, and integral gain is K_i. The transfer function would typically represent the integrator $\frac{1}{s}$, assuming it integrates concerning time. Figure 4 shows the complete phase-locked loop configuration.

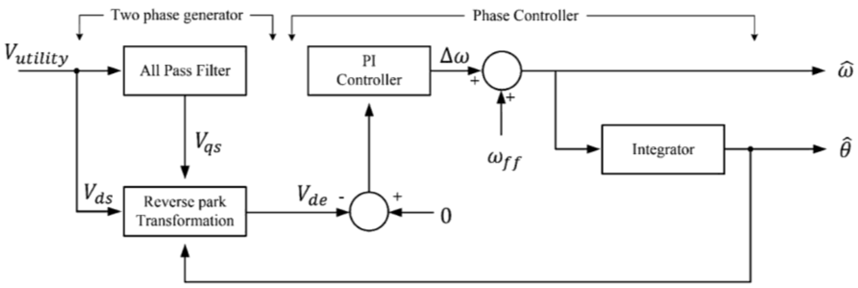

Figure 3. PLL block diagram for a single-phase PV inverter controller

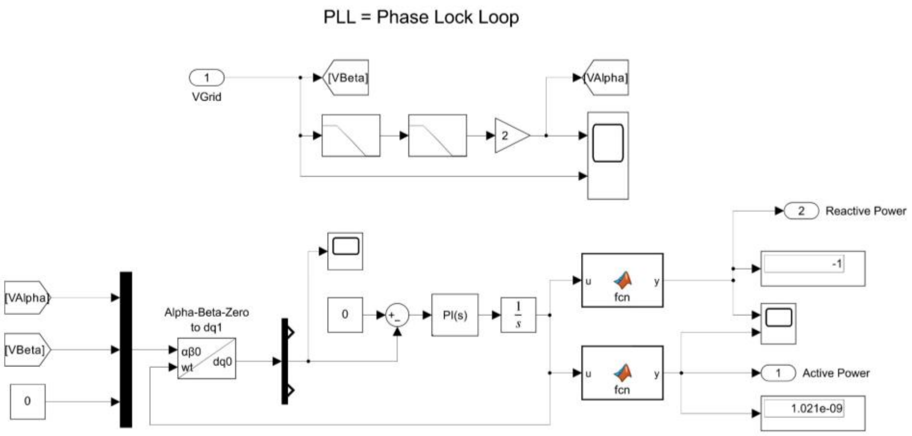

Figure 4. Phase lock loop control blocks in the MATLAB

2.6. Design of feedback control

As depicted in Figure 5, the inverter’s control architecture integrates a Feedback Controller connected to the input of the PLL control system. This PLL is crucial for controlling and synchronizing the inverter's firing angle by providing control input from the grid. The controller used is a sliding mode controller, a non-linear control method designed to influence the dynamics of a non-linear system through discontinuous control actions. The output from the sliding mode controller is directed to both the inverter and the boost inverter switch, transforming the inverter into a feedback-controlled system that is synchronized with the grid voltage. The parameters set for this system in Figure 5 are specified as follows: the proportional gain K_{p1} is set at 2.03, the derivative gain K_d at 0.0002, the second proportional gain K_{p2} at 1, and the integral gain K_i at 3,142. These settings are calibrated to optimize the system's response and efficiency, ensuring robust control and stable synchronization with the grid's fluctuating dynamics. This configuration underlines the complexity and precision required in designing control systems for modern inverters, aiming for maximum efficiency and reliability in grid-connected applications.

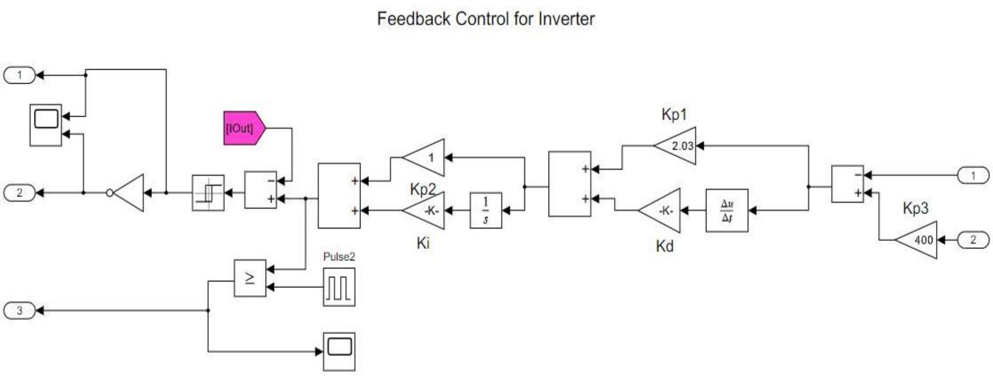

Figure 5. Sliding mode controller for feedback control loop for inverter

3. RESULTS AND DISCUSSION

In the context of the parameters discussed earlier, the design of the inverter was meticulously prepared using MATLAB, as illustrated in Figure 6. To ensure the accuracy and functionality of the inverter, it was evaluated under five distinct scenarios, each aimed at testing specific performance aspects. These scenarios were designed to examine the response of the inverter to grid fluctuations, efficiency in power conversion, and stability under dynamic loads, ensuring a comprehensive assessment of its capabilities.

The first case focused on analyzing the standalone system performance without PLL and grid connection. In the second case, the transient response of the PLL under optimal grid supply conditions was examined to assess its synchronization accuracy. The third case involved evaluating the behavior of the inverter in the event of a grid supply loss, which is crucial for determining its resilience and ability to handle unexpected disconnections. The fourth case studied the inverter’s response to frequency disturbances in the grid supply, ensuring that the system remains stable under fluctuating conditions. Finally, the fifth case investigated the impact of amplitude variations in the grid supply, testing the inverter’s ability to regulate voltage effectively.

Each of these cases presented unique challenges that the inverter needed to handle, verifying its robustness and adaptability in real-world applications. The results obtained from these tests provided critical insights into the inverter overall reliability and efficiency. By analyzing its performance across different operating conditions, necessary optimizations and refinements could be made to enhance its stability and effectiveness. This rigorous evaluation methodology ensures that the inverter is well-suited for seamless integration with solar PV systems, offering a dependable and efficient solution for grid-connected renewable energy applications.

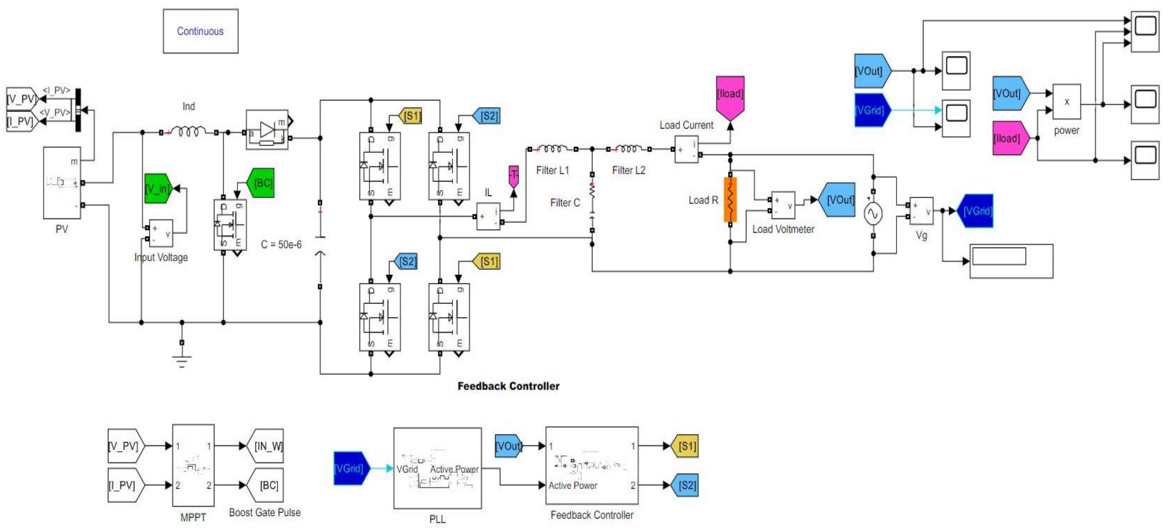

Figure 6. Detailed MATLAB/Simulink model of a grid-connected PV inverter with control mechanisms

3.1. Case 1: analyzing standalone system performance without PLL and grid connection

The analyses were initially conducted without a grid connection and without linking the PLL to the inverter. As observed in Figures 7(a) and 7(b), the output waveform without PLL control exhibits significant distortion and a high level of transients. This distortion is further evidenced by the harmonic content, which reaches up to 22.2% as depicted in Figure 7(b).

To address these issues and improve the quality of the output waveform, the PLL control was integrated into the system. The inclusion of PLL control aims to synchronize the inverter's output with the grid's frequency and phase, thereby significantly reducing harmonic distortion and transients. This adjustment allows the system to meet the standards for allowable harmonics, which are essential for grid compliance and efficient operation. These improvements and their effects are elaborated in the various cases discussed throughout the paper. By incorporating PLL control, the inverter's performance aligns with regulatory standards and contributes to a more stable and reliable grid-connected solar PV system. This demonstrates the critical role of PLL in enhancing inverter functionality and ensuring compatibility with the grid infrastructure.

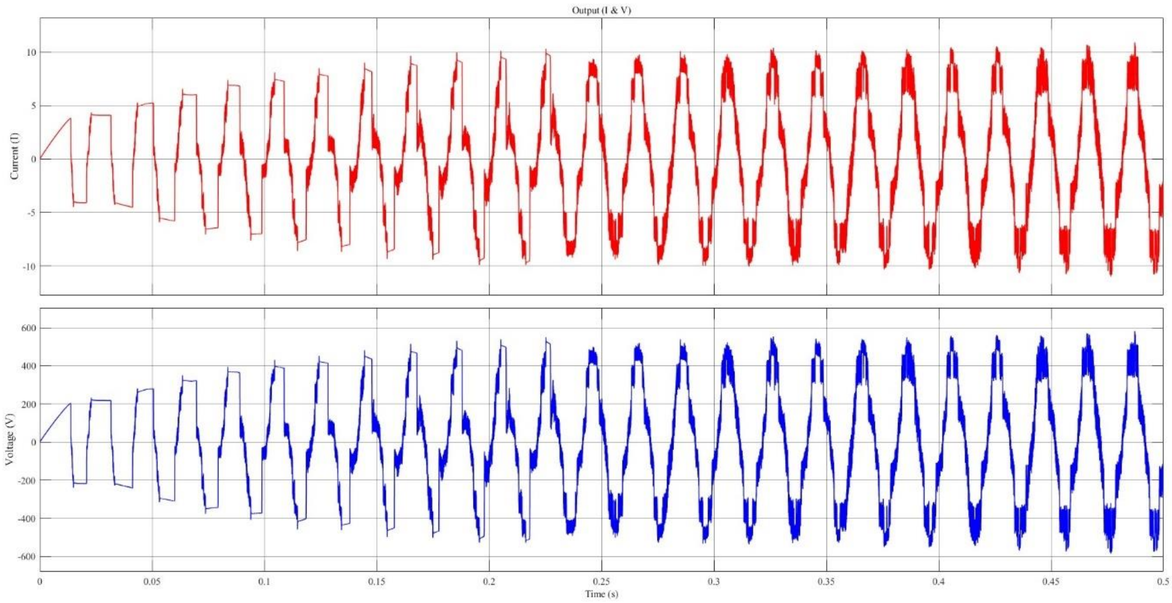

(a)

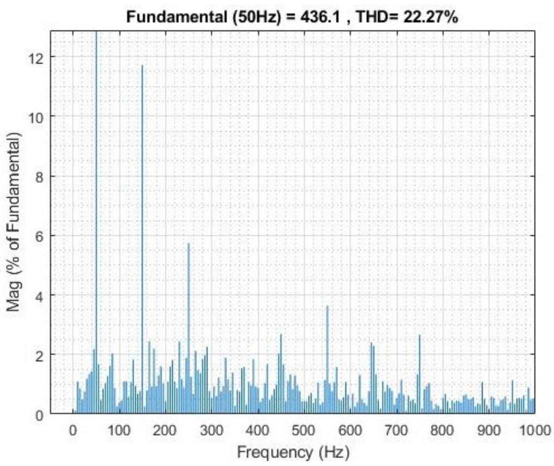

(b)

Figure 7. Voltage output and transient response of the standalone inverter without PLL (a) voltage output and transient response of the standalone inverter without PLL, and (b) transient waveform analysis

3.2. Case 2: transient response of phase-locked loops in optimum grid supply

During regular operation of the grid at optimal conditions as shown in Figure 8, where Figure 8(a) shows current and voltage output of the inverter with PLL. The frequency is stabilized at 50 Hz, the inverter performs effectively, demonstrating the effectiveness of its design. The THD is maintained at 5% at Nyquist frequency at the maximum frequency, as illustrated in Figure 8(b), these levels are compliant with the standards set by IEEE 519, which governs harmonic control in electrical power systems.

The Nyquist frequency, defined as half the sample rate of the system, represents the highest frequency that the equipment can accurately measure. The adherence to these THD values not only reflects the inverter's capability to operate efficiently under standard grid conditions but also underscores the precision of the inverter design. The integration of the PLL and feedback control plays a crucial role in this performance, ensuring that the inverter's output harmonics are well within acceptable limits. Additionally, the MPPT system maximizes power extraction from the solar panels, optimizing the overall energy production of the system. This operational efficiency confirms the correctness of the inverter's design, highlighting its capability to perform reliably and effectively in grid-connected scenarios while adhering to industry standards for power quality.

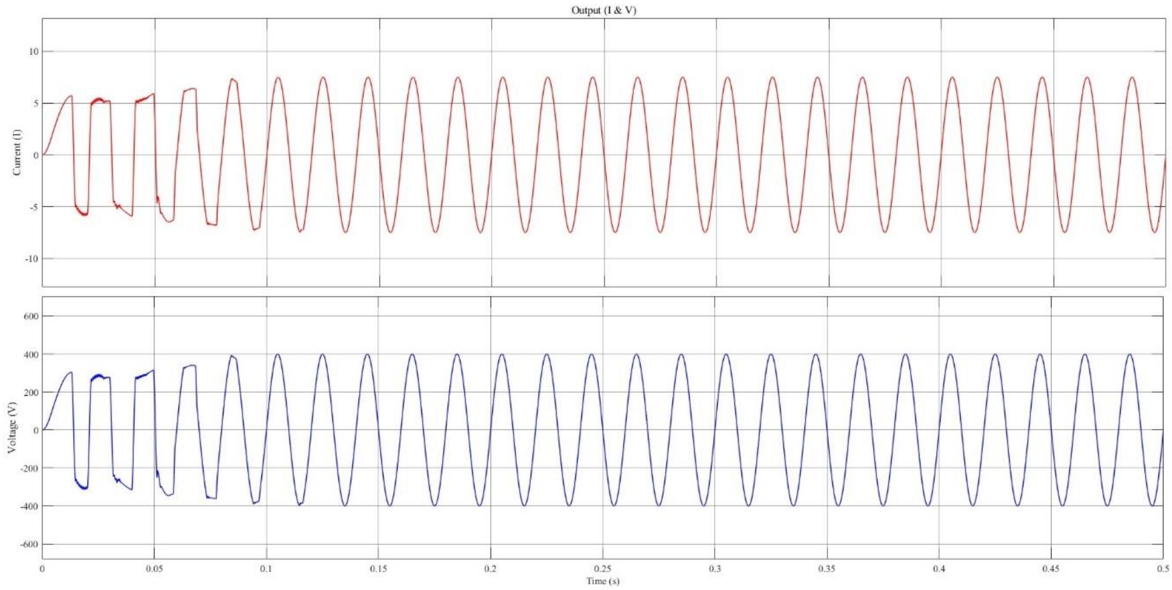

(a)

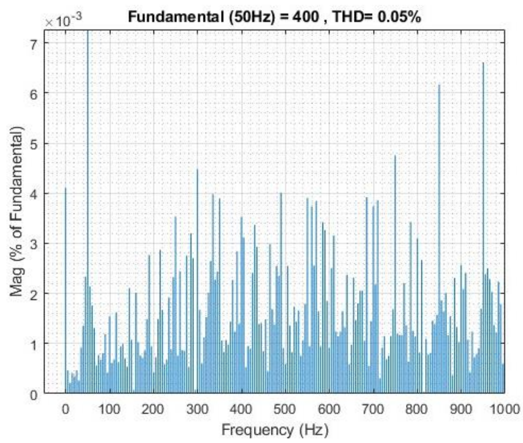

(b)

Figure 8. Transient response of phase-locked loop in optimum grid supply (a) current and voltage output of the inverter with PLL and (b) voltage transient response of the inverter in optimum grid supply

3.3. Case 3: loss of grid supply

In case 3 of the scenarios evaluated, a specific fault condition was simulated where there is a temporary interruption in the grid supply for a duration of 0.3 seconds. The grid frequency remains constant at 50 Hz throughout the test, and the grid disconnects and subsequently reconnects after 0.3 seconds. This transient event and its impact on the inverter's performance are illustrated in Figure 9.

The depiction in Figure 9(a) shows two key waveforms: the red graph represents the grid supply, and the blue waveform shows the voltage output from the inverter. This blue waveform is crucial as it demonstrates the response of the inverter, controlled by the PLL and feedback mechanisms, during and after the grid fault. The blue waveform behavior during the fault indicates how effectively the PLL and feedback control manage the inverter's operation amidst grid inconsistencies. The PLL role is to ensure the inverter output remains synchronized with the grid frequency even when the grid supply is unstable or momentarily unavailable. This is critical for maintaining the stability of the entire system and minimizing the impact of disturbances on connected loads. The ability of the inverter to continue operating effectively during this fault, as evidenced by the controlled and stable output voltage, is a testament to the robustness of the inverter’s design and control schemes. Figure 9(b) shows the power delivery to the load and the grid where it highlights the system capability to handle grid disturbances while maintaining operational continuity, ensuring that power delivery is sustained even under challenging conditions. This resilience is essential for systems that must operate reliably in environments where grid stability cannot always be guaranteed.

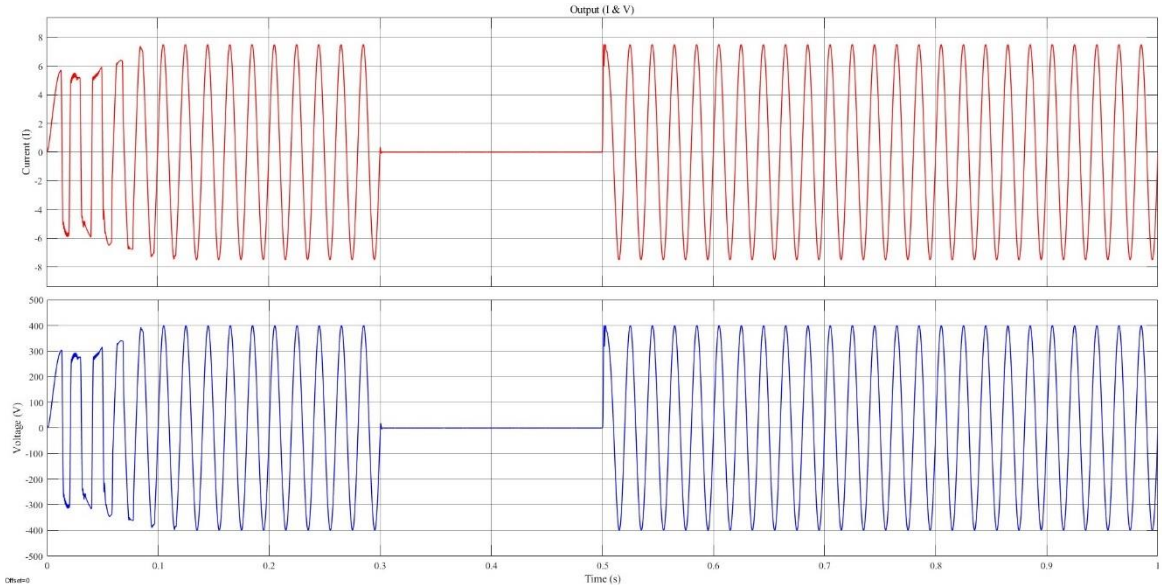

(a)

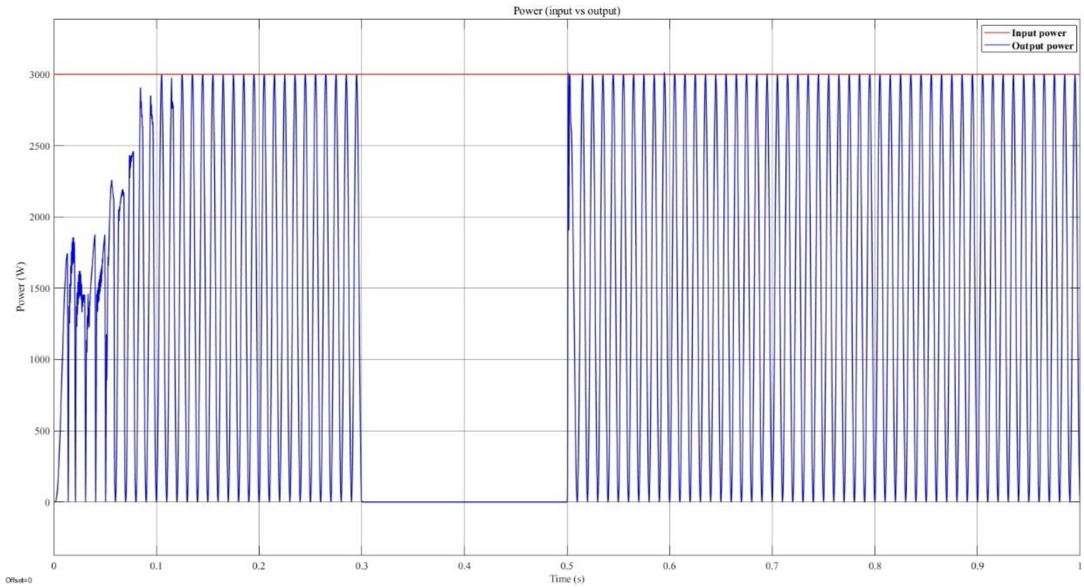

(b)

Figure 9. Inverter response to grid interruption (a) current and voltage output of the inverter during grid interruption and (b) output and input power of the inverter

3.4. Case 4: frequency disturbance in the grid supply

In this scenario the grid experiences a sequence of disturbances that are meticulously simulated to assess the inverter's robustness and its control systems under varying conditions. Initially, there is a grid disturbance lasting 0.3 seconds with the grid frequency dipping slightly to 49.5 Hz. This is followed by a brief period where the frequency stabilizes back to the standard 50 Hz for 0.34 seconds. Subsequently, another disruption occurs from 0.38 seconds, during which the grid frequency escalates to 50.5 Hz as shown in Figure 10.

Figure 10(a) captures these fluctuations, with the red graph illustrating the grid supply voltage and the blue waveforms indicating the inverter’s response. This visual representation allows for a clear observation of how the inverter, guided by the PLL and its feedback mechanisms, reacts to the varying grid conditions. The inverter response, as shown by the blue waveforms, is critical as it demonstrates the effectiveness of the PLL in managing the output frequency and voltage despite external faults from the grid side. The ability of PLL to swiftly adjust to these changes is crucial for maintaining power quality as shown in Figure 10(b) and system stability. The scenario tests the limits of the inverter's control system to ensure that, even in the face of rapid and significant frequency variations, the system can continue to operate effectively, minimizing any potential disruptions to connected loads. This case serves as a perfect examination of how well the inverter and its PLL can handle real-world grid disturbances, ensuring that the output remains stable and within acceptable limits despite external challenges. This capability is essential for maintaining reliable operation in environments with frequent grid fluctuations

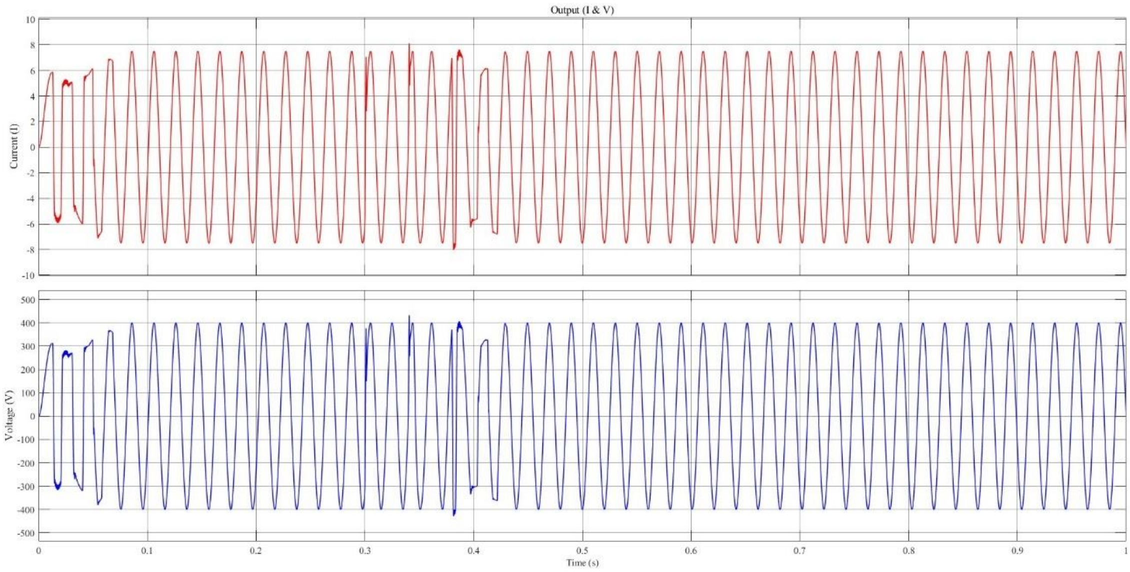

(a)

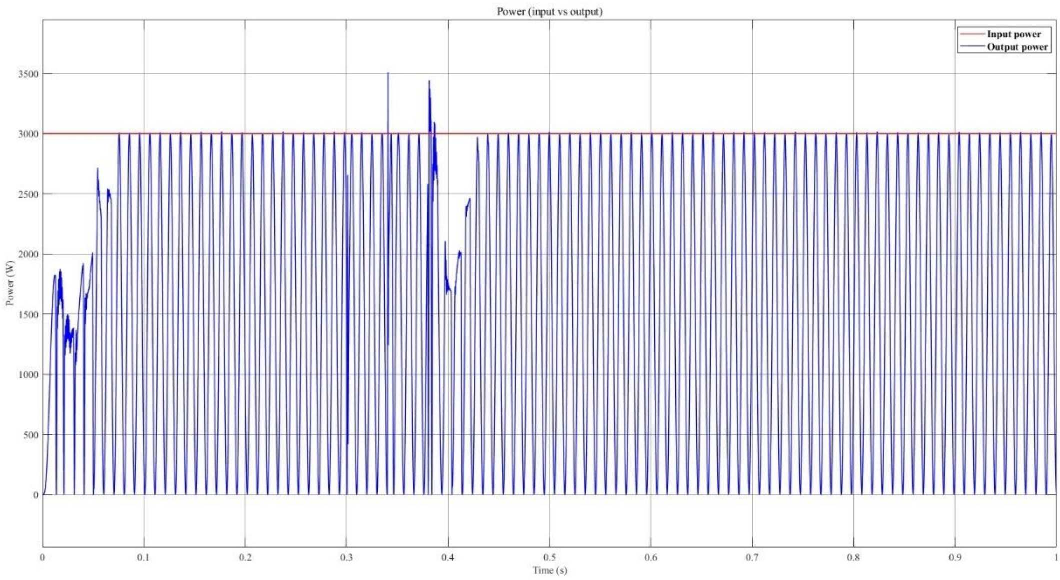

(b)

Figure 10. Inverter response to frequency disturbance in grid supply (a) current and voltage output of the inverter under variable grid frequency and (b) output and input power of the inverter

3.5. Case 5: amplitude change in the grid supply

The grid undergoes a sequence of voltage disturbances specifically designed to test the inverter's response and resilience under non-ideal conditions. Initially, for the first 0.3 seconds, the grid operates at a peak voltage of 311 V, which is considered normal. Subsequently, from 0.3 seconds to 0.6 seconds, there is a disturbance where the grid peak voltage increases by 10%. After 0.6 seconds, the voltage then decreases by 10% as shown in Figure 11(a).

Figure 11(a) visually captures these fluctuations with the red graph representing the grid supply voltage and the blue waveforms depicting the inverter's response. This response is crucial as it illustrates how the PLL manages the output frequency and voltage of the inverter in reaction to these external voltage disturbances from the grid. The PLL role here is vital; it must adjust the inverter's settings in real-time to cope with the increased and decreased voltages to maintain stability and continuity of power. This includes managing the inverter's output to ensure it does not reflect the grid's volatility but instead maintains a steady and reliable output. The ability of PLL to adapt quickly to such changes is essential for protecting the system and connected loads from potential harm caused by fluctuating voltages. The case demonstrates the effectiveness of the PLL and the overall inverter design in handling significant and rapid changes in grid voltage, showcasing the system capability to sustain operational integrity and performance even under challenging grid conditions. This ensures that the inverter can reliably support grid stability and provide a consistent power supply as shown in Figure 11(b), which is critical for both residential and commercial applications that depend on stable and reliable energy delivery.

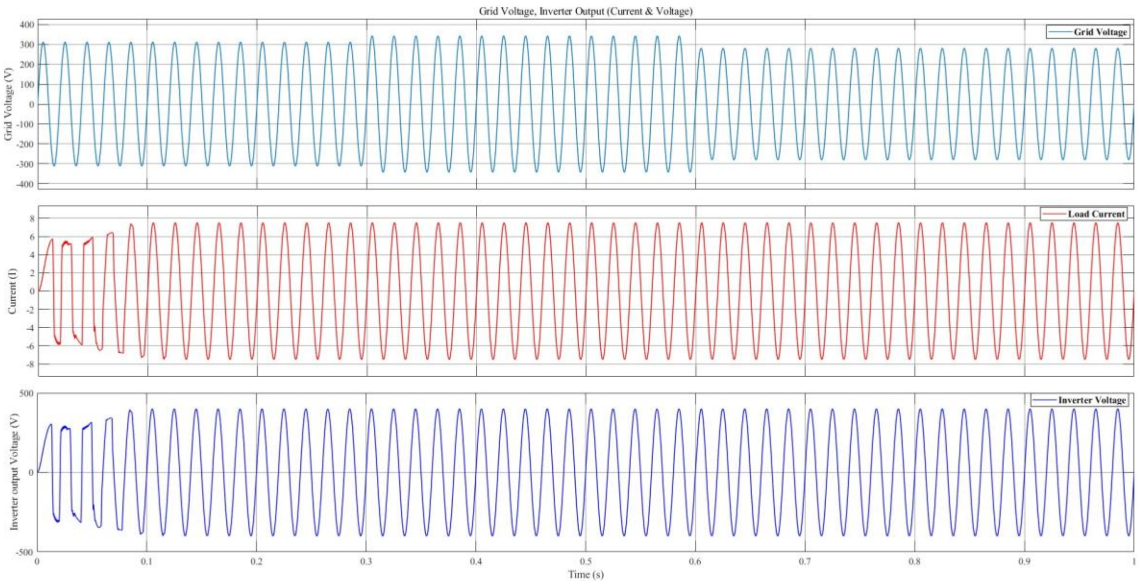

(a)

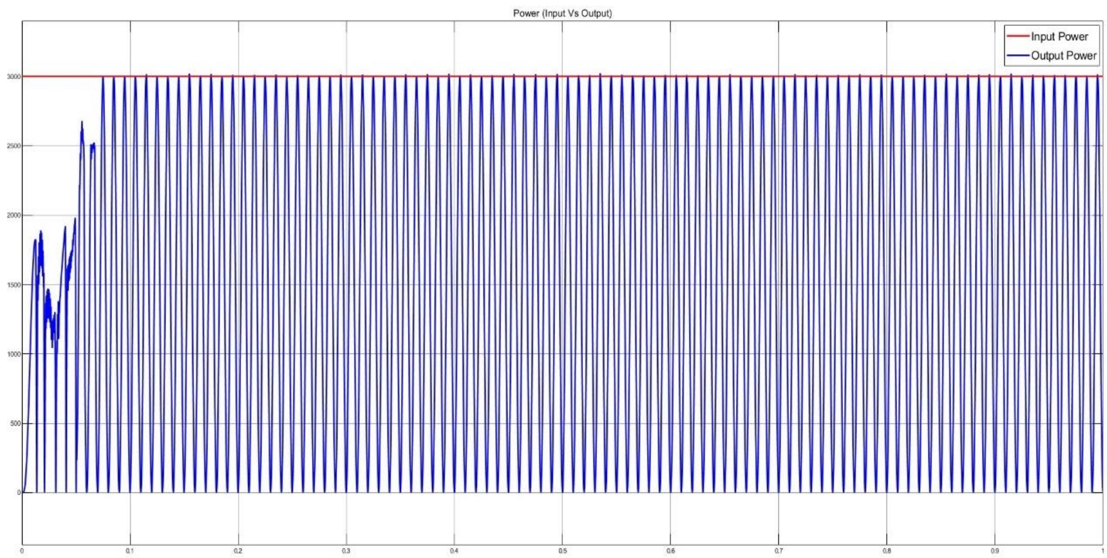

(b)

Figure 11. Inverter response to amplitude change in grid supply (a) current and voltage output of the inverter under variable amplitude in grid voltage and (b) output and input power of the inverter

4. CONCLUSION

This paper has introduced a high-frequency GaN-based inverter designed for seamless integration with AC grids. It features an innovative phase-locked loop controller utilizing sliding mode control, enhancing the smooth injection of power from photovoltaic sources into the grid. The integration of sliding mode control with phase-locked loop addresses common irregularities effectively, offering a robust solution against grid disturbances such as supply amplitude fluctuations, disconnections, and frequency variations.

The inverter has been rigorously tested under various challenging scenarios documented in literature, demonstrating its resilience and superior performance. Compared to traditional inverter designs that lack advanced control mechanisms or rely solely on proportional integral control, this GaN-based inverter significantly reduces total harmonic distortion, enhancing power quality and grid compatibility. The successful integration of PV systems with AC grids is crucial for maximizing solar energy utilization and promoting the sustainable development of renewable energy technologies. By overcoming significant challenges such as inefficiencies, poor power quality, and compatibility issues commonly associated with GaN devices, the proposed inverter not only contributes to enhancing the efficiency and reliability of renewable energy systems but also supports the broader adoption and sustainability of solar energy solutions. This advancement underscores the critical role of innovative inverter technologies in the evolution of energy systems towards greater reliance on renewable sources.

ACKNOWLEDGMENT

The authors would like to thank Gdańsk University of Technology, Poland, for providing the laboratory and resources for this research. This paper is the outcome of the author's Ph.D. research. It will be extended with further experimental and review paper.

FUNDING INFORMATION

This research did not receive any specific grant from funding agencies in the public, commercial, or non-profit sectors.

AUTHOR CONTRIBUTIONS STATEMENT

This journal uses the Contributor Roles Taxonomy (CRediT) to recognize individual author contributions, reduce authorship disputes, and facilitate collaboration.

Name of Author	C	M	So	Va	Fo	I	R	D	O	E	Vi	Su	P	Fu
Arsalan Muhammad Soomar	✓	✓	✓	✓	✓	✓	✓	✓	✓	✓	✓		✓	✓
Piotr Musznicki	✓						✓			✓		✓	✓	

C : **C**onceptualization
M : **M**ethodology
So : **So**ftware
Va : **Va**lidation
Fo : **Fo**rmal analysis
I : **I**nvestigation
R : **R**esources
D : **D**ata Curation
O : Writing - **O**riginal Draft
E : Writing - Review & **E**diting
Vi : **Vi**sualization
Su : **Su**pervision
P : **P**roject administration
Fu : **Fu**nding acquisition

CONFLICT OF INTEREST STATEMENT

The authors declare that they have no known competing financial, personal, or professional interests that could have appeared to influence the work reported in this paper.

DATA AVAILABILITY

The data that supports the findings of this study is available from the corresponding author, AMS, upon reasonable request.

REFERENCES

[1] M. N. H. Khan, M. Forouzesh, Y. P. Siwakoti, L. Li, T. Kerekes, and F. Blaabjerg, "Transformerless inverter topologies for single-phase photovoltaic systems: A comparative review," *IEEE Journal of Emerging and Selected Topics in Power Electronics*, vol. 8, no. 1, pp. 805–835, Mar. 2020, doi: 10.1109/jestpe.2019.2908672.

[2] A. Reatti, F. Corti, A. Tesi, A. Torlai, and M. K. Kazimierczuk, "Effect of parasitic components on dynamic performance of power stages of DC-DC PWM buck and boost converters in CCM," in *2019 IEEE International Symposium on Circuits and Systems (ISCAS)*, May 2019, pp. 1–5, doi: 10.1109/ISCAS.2019.8702520.

[3] S. Singh, C. Perera, G. J. Kish, and J. Salmon, "Low harmonic loss PWM for a dual inverter drive using a floating capacitor inverter," in *2019 IEEE Energy Conversion Congress and Exposition (ECCE)*, Sep. 2019, pp. 5981–5988, doi: 10.1109/ECCE.2019.8912545.

[4] B. Parida, S. Iniyan, and R. Goic, "A review of solar photovoltaic technologies," *Renewable and Sustainable Energy Reviews*, vol. 15, no. 3, pp. 1625–1636, Apr. 2011, doi: 10.1016/j.rser.2010.11.032.

[5] J. Knight, S. Shirsavar, and W. Holderbaum, "An improved reliability Cuk based solar inverter with sliding mode control," *IEEE Transactions on Power Electronics*, vol. 21, no. 4, pp. 1107–1115, Jul. 2006, doi: 10.1109/TPEL.2006.876786.

[6] A. Kchaou, A. Ayadi, A. Naamane, N. M'Sirdi, and Y. Koubaa, "An adaptive sliding mode control based maximum power point tracking method for a PV stand-alone system," in *2017 6th International Conference on Systems and Control (ICSC)*, May 2017, pp. 69–74, doi: 10.1109/ICoSC.2017.7958702.

[7] L. Liu, Y. Zhao, Y. Yin, and J. You, "Current sensor-less control for boost DC-DC converter based on switched observer," in *IECON 2018 - 44th Annual Conference of the IEEE Industrial Electronics Society*, Oct. 2018, pp. 1122–1127, doi: 10.1109/IECON.2018.8591651.

[8] Q. Huang, A. Q. Huang, R. Yu, P. Liu, and W. Yu, "High-efficiency and high-density single-phase dual-mode cascaded buck–boost multilevel transformerless PV inverter with GaN AC switches," *IEEE Transactions on Power Electronics*, vol. 34, no. 8, pp. 7474–7488, Aug. 2019, doi: 10.1109/tpel.2018.2878586.

[9] Y. Fan, G. Li, and W. Gao, "Integration control strategy of IPOS DC step-up type photovoltaic power plant via MMC-HVDC," in *2019 IEEE 8th International Conference on Advanced Power System Automation and Protection (APAP)*, Oct. 2019, pp. 1068–1073, doi: 10.1109/APAP47170.2019.9224806.

[10] J. Khazaei, Z. Tu, A. Asrari, and W. Liu, "Feedback linearization control of converters with LCL filter for weak AC Grid integration," *IEEE Transactions on Power Systems*, vol. 36, no. 4, pp. 3740–3750, Jul. 2021, doi: 10.1109/TPWRS.2021.3049324.

[11] M. Rivera, J. Riveros, and P. Wheeler, "Predictive current control strategies for grid connected NPC converters," in *2021 IEEE Congreso Estudiantil de Electrónica y Electricidad (INGELECTRA)*, Nov. 2021, pp. 1–6, doi: 10.1109/INGELECTRA54297.2021.9748074.

[12] L. Guanghua *et al.*, "Improved maximum power point tracking algorithms by using numerical analysis techniques for photovoltaic systems," *Results in Engineering*, vol. 21, p. 101740, Mar. 2024, doi: 10.1016/j.rineng.2023.101740.

[13] Y. C. Lin *et al.*, "Gallium nitride (GaN) high-electron-mobility transistors with thick copper metallization featuring a power density of 8.2 W/mm for Ka-Band applications," *Micromachines*, vol. 11, no. 2, p. 222, Feb. 2020, doi: 10.3390/mi11020222.

[14] H. Hu, S. Harb, N. Kutkut, I. Batarseh, and Z. J. Shen, "A review of power decoupling techniques for microinverters with three different decoupling capacitor locations in PV systems," *IEEE Transactions on Power Electronics*, vol. 28, no. 6, pp. 2711–2726, Jun. 2013, doi: 10.1109/TPEL.2012.2221482.

[15] Y. Zhang, Z. Dai, and Y. Fang, "Voltage feed forward shunt active power filter based on double loop control," in *2021 International Conference on Power System Technology (POWERCON)*, Dec. 2021, pp. 1251–1256, doi: 10.1109/POWERCON53785.2021.9697468.

[16] S. Shaikh *et al.*, "Modified sliding mode control for seamless integration of P.V. energy in A.C. grid," *Energy Reports*, vol. 12, pp. 673–686, Dec. 2024, doi: 10.1016/j.egyr.2024.06.062.

[17] A. M. Soomar and P. Musznicki, "Design of the LLC filter for AC grid-based converter," in *2024 IEEE 18th International Conference on Compatibility, Power Electronics and Power Engineering (CPE-POWERENG)*, Jun. 2024, pp. 1–6, doi: 10.1109/cpe-powereng60842.2024.10604367.

[18] A. Brahim, Y. Soufi, D. Ounnas, and D. Guiza, "Fuzzy logic control of a photovoltaic systemconnected to grid," in *2022 5th International Conference on Power Electronics and their Applications (ICPEA)*, Mar. 2022, pp. 1–6, doi: 10.1109/ICPEA51060.2022.9791172.

[19] A. Reznik, M. G. Simoes, A. Al-Durra, and S. M. Muyeen, "LCL filter design and performance analysis for grid-interconnected systems," *IEEE Transactions on Industry Applications*, vol. 50, no. 2, pp. 1225–1232, Mar. 2014, doi: 10.1109/TIA.2013.2274612.

[20] D. Pavkovic, P. Kristovic, M. Hrgetic, A. Komljenovic, and V. Uzarevic, "Single phase AC inverter current PR control with auxiliary PI controller for DC current suppression," in *IEEE EUROCON 2017 -17th International Conference on Smart Technologies*, Jul. 2017, pp. 324–329, doi: 10.1109/EUROCON.2017.8011129.

[21] L. Yang, X. He, A. Chang, and S. Liu, "Analysis and design of L + LCL-filtered dual-frequency single-phase grid-connected inverter," *IET Power Electronics*, vol. 13, no. 7, pp. 1416–1425, May 2020, doi: 10.1049/iet-pel.2019.1194.

[22] R. Xu, L. Xia, J. Zhang, and J. Ding, "Design and research on the LCL filter in three-phase PV grid-connected inverters," *International Journal of Computer and Electrical Engineering*, pp. 322–325, 2013, doi: 10.7763/IJCEE.2013.V5.723.

[23] M. Liserre, F. Blaabjerg, and S. Hansen, "Design and control of an LCL-filter-based three-phase active rectifier," *IEEE Transactions on Industry Applications*, vol. 41, no. 5, pp. 1281–1291, Sep. 2005, doi: 10.1109/TIA.2005.853373.

[24] C. Zhang, X. Wang, and F. Blaabjerg, "Analysis of phase-locked loop influence on the stability of single-phase grid-connected inverter," in *2015 IEEE 6th International Symposium on Power Electronics for Distributed Generation Systems (PEDG)*, Jun. 2015, pp. 1–8, doi: 10.1109/PEDG.2015.7223089.

[25] B. Yu, "An improved frequency measurement method from the digital PLL structure for single-phase grid-connected PV applications," *Electronics*, vol. 7, no. 8, p. 150, Aug. 2018, doi: 10.3390/electronics7080150.

BIOGRAPHIES OF AUTHORS

Arsalan Muhammad Soomar has received the M.E. and B.E. degrees in power from the Faculty of Electrical Engineering, Mehran University of Engineering and Technology. He is currently enrolled in a Ph.D. degree from the Gdańsk University of Technology (Gdańsk Tech), Gdańsk, Poland, in the Faculty of Power Electronics from the Faculty of Electrical and Control Engineering. where he is involved in power electronics. His research interests include power, renewable energy, modeling and controlling of power electronics converters, and electrical machines. He can be contacted at email: arsalan.muhammad.soomar@pg.edu.pl.

Piotr Musznicki was born in Slupsk, Poland, in 1976. He received the M.Sc. and Ph.D. degrees in power electronics from the Faculty of Electrical and Control Engineering, Gdańsk University of Technology (Gda´nsk Tech), Gdańsk, Poland, in 2001 and 2006, respectively, and the Ph.D. degree from the Laboratoire d'Electrotechnique de Grenoble, Grenoble Institute of Technology, Grenoble, France, in 2006. He is currently professor with the Gdańsk Tech, where he is involved in power electronics. His research interests include electromagnetic compatibility, modeling and controlling of power electronics converters, electrical machines, and digital signal processing. He can be contacted at email: piotr.musznicki@pg.edu.pl.